ISSN 2070-0482, Mathematical Models and Computer Simulations, 2011, Vol. 3, No. 3, pp. 388–397. © Pleiades Publishing, Ltd., 2011.
Original Russian Text © P.Kh. Atanasova, T.L. Boyadjiyev, Yu.M. Shukrinov, Ye.V. Zemlyanaya, 2011, published in Matematicheskoe Modelirovanie, 2010, Vol. 22, No. 11, pp. 49–64.

# Numerical Modeling of Long Josephson Junctions in the Frame of the Sine–Gordon Double Equation

**P. Kh. Atanasova*, T. L. Boyadjiyev, Yu. M. Shukrinov**, and Ye. V. Zemlyanaya*****

*Joint Institute for Nuclear Research, Dubna 141980, Russia*

**e-mail: poli@jinr.ru*

***e-mail: shukrinv@theor.jinr.ru*

****e-mail: Elena@jinr.ru*

Received February 1, 2010

**Abstract**—The aim of this work is the mathematical modeling of static distributions of the magnetic flow in long Josephson junctions (JJ), taking into account the second harmonic in the decomposition of the Josephson current and the sequential comparison of the results with the conventional model. For the analysis of stability, each concrete distribution of magnetic current in the junction is put into relationship with the Sturm–Liouville spectral problem; the nullification of its minimal eigenvalue indicates the bifurcation distribution by one of the problem parameters. The corresponding nonlinear boundary problem is numerically solved by a continuous analog of the Newtonian method with the spline-collocation scheme for linearized problems at each Newtonian iteration. The main distributions of the magnetic flow have been found and their stability against changes of model parameters investigated. The obtained results were compared with the results of the JJ conventional model of the superconductor–insulator–superconductor type.

*Keywords*: long Josephson junctions, fluxon solutions, stability, Newtonian scheme, spline-collocation

**DOI:** 10.1134/S2070048211030033

## 1. INTRODUCTION

Physical events in the Josephson junctions (JJ) are the basis of modern superconducting electronics. For JJ of the SIS (superconductor–insulator–superconductor) type, the current–phase dependence is a sinusoidal function. This model is described by the sine–Gordon (SG) equation. At decreased barrier transparency, this dependence weakens, when it can be taken as the Fourier–decomposition [1]. For many applications the contribution of the second harmonic is important; for example, in contacts of the SNISN and SFIFS type where $N$ denotes the layer of normal metal and $F$ the layer of metal ferromagnetic [2]. Various physical mechanisms are responsible for its sign. Thus, the collapse of Cooper pairs by the current leads to a positive sign, whereas the SF and SN finite transparency to its sign being negative [3].

If the second harmonic is taken into account, it substantially affects the distribution of the magnetic flow in JJ. However, no detailed investigations of the basic distributions in JJ, taking into account the sec-

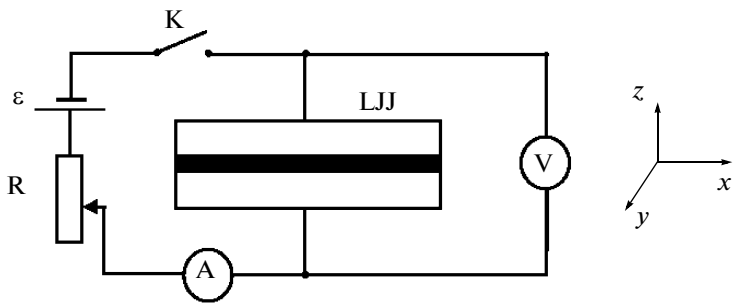


**Fig. 1.** Scheme of a long CD.

ond harmonic and their stability against the change in the JJ parameters, have been performed so far. They are the object of research in this article.

## 2. PROBLEM

Figure 1 shows the scheme of a long JJ. In its simplest form, the JJ is a "sandwich" of two layers of superconducting metals which are divided by a thin dielectric layer (tunnel barrier). The contact is in the homogenous magnetic field $h_e$ directed along the $Y$ axis. The current source $\varepsilon$ is applied to the system. In the Josephson (static) regime [4], the voltage between the superconducting layers measured by a device is $V = 0$, and in the dynamic and, in particular, resistive regime the voltage is $V \neq 0$. In the considered case of the long JJ, the sizes of the contact by the $Y$ and $Z$ axes are negligibly small and the magnetic flow $\varphi$ in the contact depends only on $x$.

The total flow through JJ has a component called supercurrent (Josephson current) $I_s$ [5]. The dependence of the $I_s$ value on the difference between the phases of wave functions of superconducting electrodes can in most cases be thought of as odd-numbered, strictly $2\pi$-periodic [6] and, therefore, presentable as a series by sines

$$I_s = I_c \sin\varphi + \sum_{m=2}^{\infty} I_m \sin m\varphi. \tag{2.1}$$

The basic amplitude $I_c$, like also the higher amplitudes $I_m$, depends on the geometry, materials, and technology of contact manufacturing [1, 7].

The exact theory [6] shows that in most cases it is possible to ignore all terms in (2.1), except for the first one, which leads to the conventional model $I_s = I_c \sin\varphi$. However, there exist real physical situations for JJ, in the simulation of which, one needs to take into account not only the first but also the higher terms in decomposition (2.1) (see, for example [1, 7–9]. In particular, limiting oneself to two items in (2.1), it is easy to show [8] that in the statistical regime of contact operation [5], the dimensionless distribution of the magnetic flow $\varphi(x)$ along axis $X$ (see Figure 1) satisfies the double sine–Gordon (2SG) equation:

$$-\varphi'' + a_1 \sin\varphi + a_2 \sin 2\varphi - \gamma = 0, \quad x \in (-l, l). \tag{2.2}$$

All values here and below are dimensionless (the ways of bringing them to the dimensionless form are found, for example, in [4] and [5, 10]). The dashed lines denote differentiation by coordinate $x$; $l$ is the half length of the contact; the value $\gamma$ denotes the external current and amplitudes $a_1$ and $a_2$ correspond to the first two coefficients in the total Fourier decomposition (2.1).

Equations of type (2.2) are encountered in a number of problems of physics; in particular, in modeling the distribution of spin waves in anisotropic spin liquids, and in nonlinear optics (distribution of ultrashort impulses in a resonance fivefold degenerate medium) [1–3, 7].

The issue of analytical solutions (2.2) on the infinite interval ($l \to \infty$) with a null external current $\gamma$ has been discussed in the literature in detail (for example, [11]).

In the case of the overlap-contact of a finite length for Eq. (2.2), the boundary problem is stated with boundary conditions

$$\varphi'(\pm l) = h_e, \tag{2.3}$$

where $h_e$ is the external magnetic field directed along the $Y$ axis.

The problem in (2.2) and (2.3) includes five parameters $p = (l, h_e, \gamma, a_1, a_2)$. Accordingly, any solution depends, in addition to the coordinate $x$, on the vector of the parameters $p$: $\varphi = \varphi(x, p)$ (hereinafter, the dependence on $p$ will be written only where required). Therefore, all values determined through the solutions of problem (2.2) and (2.3) will also be functions of $p$.

Physical experiments show that with an increase of the external current $\gamma$ by module, there is a critical value $\gamma_{cr}$, at which the contact enters the dynamic regime of operation [5]. From the mathematical viewpoint, this transition can be considered [10] as a loss of stability (bifurcation) by some of the static solutions $\varphi(x)$ of the problem in (2.2) and (2.3) with variation of $\gamma$. The minimal eigenvalue (MEV) $\lambda_0$ of the corresponding Sturm–Liouville problem (SLP)

$$-\psi'' + q(x)\psi = \lambda\psi, \quad x \in (-l; l), \tag{2.4a}$$

$$\psi'(\pm l) = 0, \tag{2.4b}$$

with potential $q(x, p) = a_1 \cos\varphi + 2a_2 \cos 2\varphi$ is nullified.

In the general case, the value $\lambda_0(p)$ lets one judge the stability of solutions $\varphi(x)$. If $\lambda_0(p) > 0$, then the corresponding solution is stable. With $\lambda_0(p) < 0$, the solution is unstable, and $\lambda_0(p) = 0$ corresponds to bifurcation of the solution in the given point of the space of the model parameters.

It should be noted that Eqs. (2.2) and (2.3), along with SLP (2.4), ensure from the necessary and sufficient condition of the extreme of the functional of the total energy of the contact:

$$F(\varphi) = \int_{-l}^{l} \left[\frac{1}{2}\varphi'^2 + 1 - q(x) - \gamma\varphi\right] dx - h_e\Delta\varphi, \tag{2.5}$$

where the value $\Delta\varphi$ is the total magnetic flow throughout the contact [10]:

$$\Delta\varphi = \varphi(l) - \varphi(-l). \tag{2.6}$$

## 3. NUMERICAL METHOD

We will consider Eqs. (2.2) and (2.3) with a fixed value of the length $2l$, external magnetic field $h_e$, external current $\gamma$, and coefficients $a_1$ and $a_2$. This is the boundary problem for the differential second order equation with Neumann conditions. In its solution, it is reasonable to use an iteration algorithm based on the continuous analogue of the Newtonian method (CANM) (see reviews [12–14].

The CANM calculation scheme applied to the solution of the JJ problem was introduced in [15]; henceforth, various modifications of the iterations on the CANM basis were successfully used in the numerical research of the JJ models in many works (see review [14] and the cited literature).

As applied to the problem at hand, CANM leads to the following sequence of iterations. Let the initial approximation $\varphi_0(x)$ be given. Then, at the $k$th step ($k = 1,2, ...$), we estimate

(1) The iteration's correction $w_k(x)$, by solving the linearized boundary problem

$$-w_k'' + q_{k-1}(x)w_k = \varphi_{k-1}'' - f_{k-1}(x), \tag{3.1a}$$

$$w_k'(-l) = -\varphi_{k-1}'(-l) + h_e, \tag{3.1b}$$

$$w_k'(l) = -\varphi_{k-1}'(l) + h_e, \tag{3.1c}$$

where $f(x) = a_1\sin\varphi + a_2\sin2\varphi - \gamma$;

(2) The next approximation to the accurate solution is

$$\varphi_k(x) = \varphi_{k-1}(x) + \tau_k w_k.$$

The iteration parameter $\tau_k$ was calculated by the Yermakov–Kalitkin [16] formula.

For simplicity, the iteration subscripts are hereinafter dropped.

In the numerical solution of linearized Eqs. (3.1), we use a differential scheme, based on the approximation of the solution by cubic splines [17]. We introduce on the interval $[-l; l]$ a homogenous grid $\{-l = x_1, x_2, \ldots x_N = l\}$ with a step of $h = x_{i+1} - x_i$, $i = 1, 2,\ldots N-1$. We look for the solution of Eqs. (3.1) in the form of a cubic spline $S(x)$ of class $C^2$, with the nodes coinciding with the nodes of the introduced grid. We arrive at the system

$$b_1w_1 + c_1w_2 = d_1, \tag{3.2a}$$

$$a_iw_{i-1} + b_iw_i + c_iw_{i+1} = d_i, \quad i = 2, 3, \ldots, N-1, \tag{3.2b}$$

$$a_Nw_{N-1} + b_Nw_N = d_N \tag{3.2c}$$

with the coefficients in the left hand part

$$b_1 = 1 + \frac{h^2}{3}q_1, \quad c_1 = -1 + \frac{h^2}{6}q_2,$$

$$a_i = -1 + \frac{h^2}{6}q_{i-1}, \quad b_i = 2 + \frac{2h^2}{3}q_i, \quad c_i = -1 + \frac{h^2}{6}q_{i+1}, \quad i = 2, 3, \ldots, N-1,$$

$$a_N = -1 + \frac{h^2}{6}q_{N-1}, \quad b_N = 1 + \frac{h^2}{6}q_N$$

and in the right hand part

$$d_1 = \varphi_2 - \varphi_1 - hh_e - \frac{h^2}{6}(2f_1 + f_2),$$

**Table 1.** Values of function φ and values σ (3.3) at the ends of interval $[-l; l)$ for the solution of the $\Phi^1$ type at $2l = 10$, $\gamma = 0$, $h_e = 2$, $a_1 = 1$, and $a_2 = 0.5$

| $N$ | $\varphi(-l)$ | $\varphi(l)$ |
|---|---|---|
| 513 | −2.295786926998205 | 8.578972227160438 |
| 1025 | −2.295516135758195 | 8.578701434682609 |
| 2049 | −2.295450140985348 | 8.578632131451062 |
| σ ≈ | 4.1 | 3.9 |

$$d_i = \varphi_{i-1} - 2\varphi_i + \varphi_{i+1} - \frac{h^2}{6}(f_{i-1} + 4f_i + f_{i+1}), \quad i = 2, 3, \ldots, N-1,$$

$$d_N = -\varphi_N + \varphi_{N-1} + hh_e - \frac{h^2}{6}(f_{N-1} + 2f_N),$$

where $\varphi_i = \varphi(x_i)$, $q_i = q(x_i)$ and $f_i = f(x_i)$.

Equations (3.2) are a three-diagonal system of $N$ linear algebraic equations for the spline values in the grid nodes. From the form of the coefficients $a_i$, $b_i$, and $c_i$, it follows that the matrix of this system has a diagonal predominance. Thus, in order to solve the system, a method of running without selecting the central element [17] is used.

According to [17], the described scheme of spline-approximation has an order of accuracy of $O(h^2)$, which is supported by test calculations on a sequence of twice condensing grids.

The problem in (2.2) and (2.3) was solved on a sequence of uniform grids with steps $h$, $h/2$, $h/4$, $h = 2l/(N-1)$, and $N = 513$. The results for solutions of the $\Phi^1$ type given in Table 1 show that the values $\sigma(x_i)$ calculated by formula

$$\sigma(x_i) = \frac{\varphi_h(x_i) - \varphi_{h/2}(x_i)}{\varphi_{h/2}(x_i) - \varphi_{h/4}(x_i)}, \quad i = 1, 2, \ldots, N, \tag{3.3}$$

are close to $2^2$, which corresponds to the theoretical order of accuracy $O(h^2)$ of the considered spline-collocation scheme on a uniform grid.

For the SLP (2.4) approximation, three-point finite-difference formulas of the second order [18] are used. In the resolution of problem (2.4), a linear algebraic problem for eigenvalues of type

$$A\psi_h = \lambda\psi_h,$$

is put in the relationship, where the vector is $\psi_h = (\psi(x_1), \psi(x_2), \ldots, \psi(x_N))^T$ and $A$ is the tridiagonal matrix. For calculation of the first several eigenvalues of the obtained matrix $A$, standard subprogram [19] is used.

## 4. NUMERICAL RESULTS

For the sake of clarity, we have at least briefly to dwell on some basic types of static solutions which take place in the conventional case ($a_1 = 1$, $a_2 = 0$). In the null field ($h_e = 0$), problem (2.2), (2.3) has a multitude of the Meissner (trivial, vacuum) solutions of the $\varphi(x) = \arcsin(\gamma) + 2k\pi$, $k = 0, \pm1, \pm2, \ldots$ type. The solutions stemming from the main value of the arcsin function are stable, while the rest are unstable. Hereinafter, stable and unstable Meissner solutions will be denoted as $M_0$ and $M_\pi$, respectively.

An important role in the theory is played by solutions corresponding to the vortex distributions of the magnetic flow in the contact. The simplest vortex solutions are fluxon/antifluxon solutions (we use below an abridged notation $\Phi^1$, $\Phi^{-1}$), for which in the infinite contact ($l \to \infty$) with $h_e = 0$ and $\gamma = 0$, exact analytical expressions are known [10]:

$$\Phi^{\pm}_{\infty} \equiv \varphi(x) = \arctan\exp(\pm x) + 2k\pi. \tag{4.1}$$

Here, the sign '+' corresponds to fluxon $\Phi^1$ and the sign '−' to antifluxon $\Phi^{-1}$.

In contacts of finite length, objects of type (4.1) are not fluxons in the strict meaning of the word (that is, they are not exact solutions of boundary problem (2.2), (2.3), but a number of their features, and, in particular, finite energy and dimensions, allow the practicability and convenience of this terminology.

In the JJ of a finite length of $2l$, there are also multifluxon distributions, for which the denotation of a $\varphi_n$ type are used below. Here, $n$ is the number of vortices defined as the value of the functional [14]

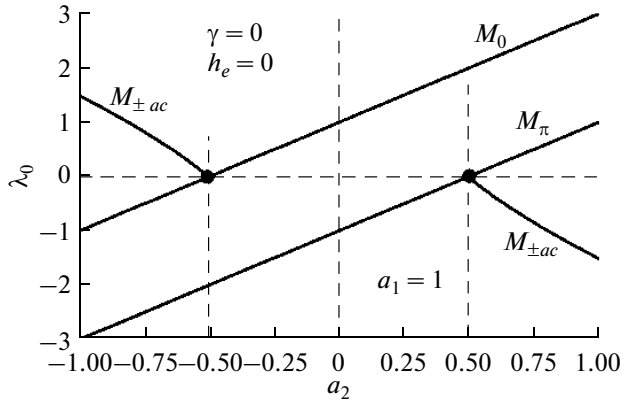


**Fig. 2.** MEV for a CD at $\gamma = 0$ and $h_e = 0$, depending on parameter $a_2$ with a fixed positive value of parameter $a_1 = 1$.

$$N[\varphi] = \frac{1}{2l\pi}\int_{-l}^{l}\varphi(x,p)dx \qquad (4.2)$$

at the point $\varphi(x, p)$. For an infinite contact, the expression in the right hand part should be understood in the sense of a limit transition.

As any solution $\varphi(x)$ of problem (2.2) and (2.3) is determined to an accuracy up to $2k\pi$, then, also the value $N(\varphi)$ is found to an accuracy of up to $2k$. The arbitrariness in the selection of integer $k$ can be used to matchvalue $N(p)$ with the value of the total magnetic flow of distribution $\Delta\varphi(p)$ in accordance with condition

$$|N[\varphi] - \Delta\varphi/2\pi| \to \min.$$

In particular, selecting $k = 0$ and $k = -1$ for solutions (4.1), it is easy to verify that $N[\Phi_\infty^\pm] = \pm 1$ and $\Delta\varphi/2\pi = \pm 1$.

If the external current is $\gamma = 0$, then for any admissible field $h_e$, the solutions $M_0$ and $M_\pi$, as well as the $n$-fluxon/antifluxon distributions $\Phi^{\pm n}$, are characterized by values $N[M_0] = 0$, $N[M_\pi] = 1$, and $N\{\Phi_\infty^{\pm n}\} = \pm n$.

### *4.1. Constant Solutions of 2SG-Equations and Their Stability*

If we take into account the second harmonic $a_2\sin 2\varphi$ in model (2.2), then for $\gamma = 0$ and $h_e = 0$, in addition to the trivial solutions $M_0$ and $M_\pi$ in the traditional case ($a_1 = 1$, $a_2 = 0$), it leads to are two other classes of solutions $\varphi = \pm\arccos(-a_1/2a_2) + 2k\pi$ (denoted as $M_{\pm ac}$). The corresponding MEV as functions of the coefficients of 2SG-equation (2.2) are

$$\lambda_0(M_0) = a_1 + 2a_2, \quad \lambda_0(M_\pi) = -a_1 + 2a_2, \quad \lambda_0(M_{\pm ac}) = (a_1^2 - 4a_2^2)/2a_2.$$

Figure 2 shows the dependences of MEV of four constant distributions (CDs) on $a_2$ with the assigned $a_1 = 1$. The vertical line $a_2 = 0$ corresponds to the trivial case. There are only two constant CDs here: $M_0$, for which $\lambda_0 = 1$, and $M_\pi$, for which $\lambda_0 = -1$. In the interval $a_2\varepsilon(-0.5; 0.5)$, the MEV signs are kept.

Points $a_2 = \pm 0.5$ are bifurcation points. With $a_2 < -0.5$, the two $M_{\pm ac}$ distributions are the only stable states. With $a_2 > 0.5$, there are also two stable solutions $M_0$ and $M_\pi$.

The exponential stability of CDs is determined by the signs of parameters $a_1$ and $a_2$ and their relationship $a_1/a_2$.

In the case $\gamma \neq 0$, the CD is $\varphi = \arcsin z + 2k\pi$, with $k = 0, \pm 1, \pm 1, \ldots$, where $\mathbf{z}$ are solutions of the algebraic biquadratic equation $4a_2^2z^4 + (a_1^2 - 2a_2^2)z^2 - 2a1\gamma\mathbf{z} + \gamma^2 = 0$.

### *4.2. Some Fluxon Solutions*

In this work, the calculations were made with the number of discrete approximation points $N = 1025$ on the interval $[-5; 5]$, with $a_1 = 1$.

**Table 2.** Some solutions at $2l = 10$, $\gamma = 0$, $h_e = 0$, and $a_2 = 0$

| Type | $\lambda_0$ | $N[\varphi]$ | $\varphi(0)/\pi$ | $\Delta\varphi/2\pi$ | $F[\varphi]/8$ |
|---|---|---|---|---|---|
| $M_0$ | 1 | 0 | 0 | 0 | 0 |
| $\Phi^{-1}$ | −0.0007 | −1 | −1 | −0.9828 | 0.9998 |
| $\Phi^1$ | −0.0007 | 1 | I | 0.9828 | 0.9998 |
| $M_\pi$ | −1 | 1 | 1 | 0 | 2.5 |

In Tables 2–4, the values are given of $\lambda_0$, the number of fluxons $N[\varphi]$, the values of distributions in the middle of interval $\varphi(0)/\pi$, the total magnetic flow $\Delta\varphi/2\pi$, and the total energy of contact $F/8$.

The values of basic physical characteristics $M_0$, $M_\pi$, and single-fluxon solutions $\Phi^{\pm 1}$ in the conventional case $\alpha_2 = 0$ are shown in Table 2. The only stable solution is $M_0(\lambda_0 = 1)$. The sin-

**Table 3.** Some solutions at $2l = 10$, $\gamma = 0$, $h_e = 0$, and $a_2 = 0.2$

| Type | $\lambda_0$ | $N[\varphi]$ | $\varphi(0)/\pi$ | $\Delta\varphi/2\pi$ | $F[\varphi]/8$ |
|---|---|---|---|---|---|
| $M_0$ | 1.4 | 0 | 0 | 0 | −0.5 |
| $\Phi^{-1}$ | −0.0003 | −1 | −1 | −0.9919 | 0.7434 |
| $\Phi^1$ | −0.0003 | 1 | 1 | 0.9919 | 0.7434 |
| $M_\pi$ | −0.6 | 1 | 1 | 0 | 2 |

**Table 4.** Some solutions at $2l = 10$, $\gamma = 0$, $h_e = 0$, and $a_2 = 0.7$

| Type | $\lambda_0$ | $N[\varphi]$ | $\varphi(0)/\pi$ | $\Delta\varphi/2\pi$ | $F[\varphi]/8$ |
|---|---|---|---|---|---|
| $M_0$ | 2.4 | 0 | 0 | 0 | −1.75 |
| $M_\pi$ | 0.4 | 1 | 1 | 0 | 0.75 |
| $\Phi^{-1}$ | −0.0001 | −1 | −1 | −0.9983 | −0.0259 |
| $\Phi^1$ | −0.001 | 1 | 1 | 0.9983 | −0.0259 |
| $M_{-ac}$ | −0.6857 | −0.7532 | −0.7532 | 0 | 2.1071 |
| $M_{ac}$ | −0.6857 | 0.7532 | 0.7532 | 0 | 2.1071 |

gle-fluxon solutions $\Phi^{\pm1}$ are shown in the next two of Table 2. For them, $\lambda_0 = -0.0007$, that is, with the null external field and with the null external current, these solutions are close to the bifurcation state but they still remain unstable. The values $\varphi(0)/\pi = \pm1$, $\Delta\varphi/2\pi \approx \pm0.98$, and $F[\Phi^{\pm1}]/8 \approx 1$ exhibit a similarity with fluxons $\Phi_\infty^{\pm1}$ in infinite contact (4.1). The last solution in Table 2 is $M_\pi$, for which $\lambda_0 = -1$. For this CD, the number of fluxons equals unity. From last column 2, it is seen that the energy of the considered solutions increases with a decline of the corresponding $\lambda_0$.

The values of the basic physical characteristics of some of the solutions with values of parameters $\gamma = 0$, $h_e = 0$, and $a_2 = 0.2$ are shown in Table 3, and with values of parameters $\gamma = 0$, $h_e = 0$, and $a_2 = 0.7$ are shown in Table 4. The only solution which always remains stable at the considered values of the parameters of the problem is the Meissner solution $M_0$. From Tables 2–4, it is seen that for CDs, $M_\pi$ is unstable with $a_2 = 0$ ($\lambda = -1$) and with $a_2 = 0.2$ ($\lambda_0 = -0.6$). With $a_2 = 0.7$, the value $\lambda_0 = 0.4$, that is, $M_\pi$ is stable. The solutions $M_{\pm ac}$ exist with $a_2 > 0.5$ (Table 4) and for these parameter values they are unstable. Of all solutions considered in Tables 2–4, the $M_{\pm ac}$ are the only ones for which the number of fluxons is not an integer. In particular, with $a_2 = 0.7$, we have $N[M_{\pm ac}] \approx \pm0.75$.

Figure 3 shows the behavior of the total energy with a change in the amplitude $a_2$ for the considered distributions in the junction with $h_e = 0$. It is clearly seen that the energy of the conventional Meissner solutions $M_0$ and $M_\pi$ decreases and the total energy $M_{\pm ac}$ increases with the increase of parameter $a_2$. The only stable solution in the field of change of parameter $a_2 \in [0; 0.5]$ and thus realizable in the experiment is the standard Meissner distribution $M_0$. With $a_2 > 0.5$, another stable state $M_\pi$ appears, then $F[M_0] < F[M_\pi]$, therefore, CD $M_0$ has a higher probability of experimental implementation.

In fairly large magnetic fields, the situation changes substantially. An example is given in Fig. 4, where the curves of the total energy dependence on $a_2$ are demonstrated only for stable distributions in the field $h_e = 0.2$. Up to values of $a_2 \approx 0.6$, only two distributions $M_0$ and $\Phi^1$ are stable. Moreover, $F[M_0] < F[\Phi^1]$ and, therefore, distribution $M_0$ is energetically preferable; that is, in the experiment, the probability of its implementation is higher than the probability to implement distributions $\Phi^1$. In the case $a_2 = 0$, a similar

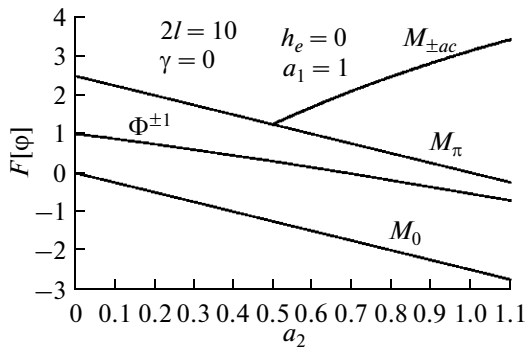


**Fig. 3.** Dependence of total energy on parameter $\alpha_2$ at fixed values $h_e = 0$, $\gamma = 0$, and $2l = 10$ for a CD and $\Phi^{\pm1}$.

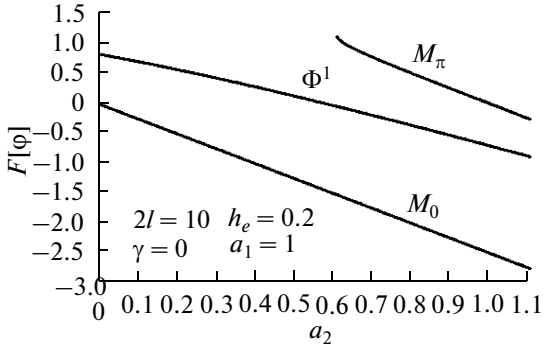


**Fig. 4.** Dependence of total energy on parameter $\alpha_2$ at fixed values $h_e = 0.2$, $\gamma = 0$, and $2l = 10$ for stable states $M_0$, $M_\pi$, and $\Phi^1$.

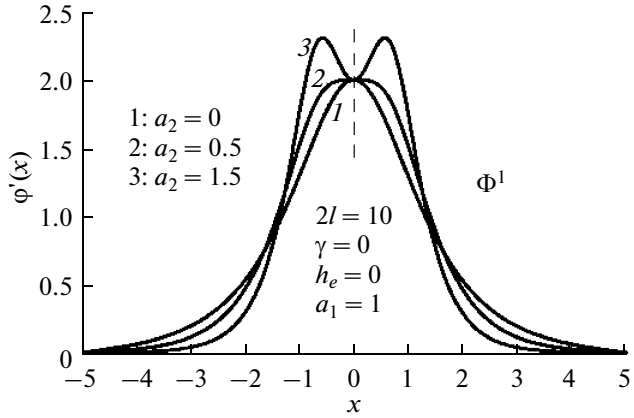


**Fig. 5.** $\Phi^1$ at $a_1 = 1$ and $\gamma = 0$. $h_e = 0$ and $2l = 10$ under a change of parameter $a_2$.

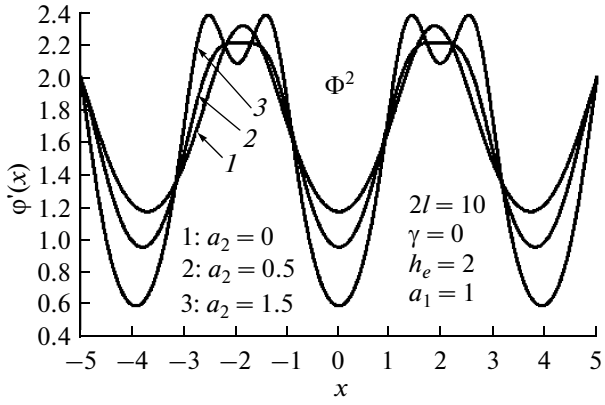


**Fig. 6.** Double-fluxon solutions $\Phi^2$ at $a_1 = 1$, $2l = 10$, and $h_e = 2$ under a change of parameter $a_2$.

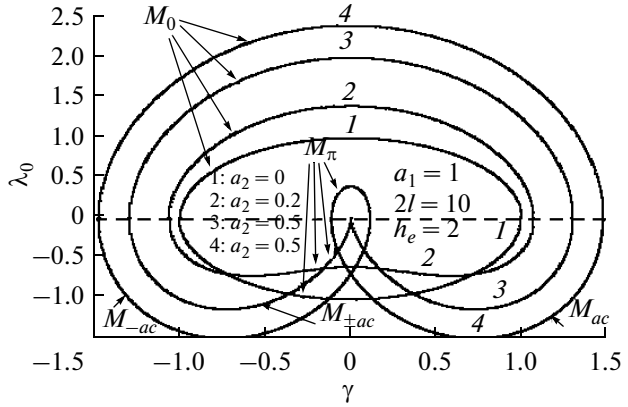


**Fig. 7.** MEV's dependence on external current $\gamma$ for a CD at fixed values $a_1 = 1$, $h_e = 0$, and $2l = 10$ and with different values of parameter $a_2$.

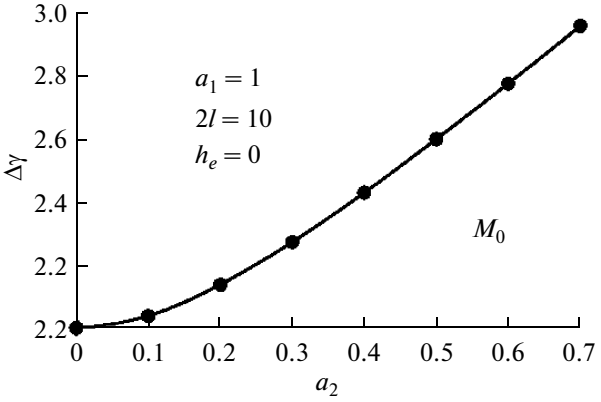


**Fig. 8.** Dependence of the field of stability by external current $\gamma$ of solution $M_0$ on parameter $a_2$ at $a_1 = 1$, $2l = 10$, and $h_e = 0$.

effect was noted in the classical work [20]. Experimental validation for contacts with microresistive inhomogeneity in the barrier layer can be found in [21].

At $a_2 > 0.6$, the solution $M_\pi$ also becomes stable at the junction. As the corresponding total energy is larger than the total energies of distributions $M_0$ and $\Phi^1$, the probability to implement $M_\pi$ in the experiment is the smallest.

Figure 5 demonstrates the deformation of derivative solutions (of the internal magnetic field) of type $\Phi^1$ under the influence of parameter $a_2$. The internal magnetic field $\varphi'(x)$, corresponding to solution $\Phi^1$, is symmetrically relative to $x = 0$ at all values of the parameter $a_2$ (Fig. 5). At $a_2 = 05$, the curve $\varphi'(x)$ has a plateau in the central neighborhood $x = 0$. A further increase of parameter $a_2$ leads to the formation of two maxima of the function $\varphi'(x)$. Hence, taking coefficient $a_2$ into account leads to a qualitative change in the apearance of the fluxons.

Let us consider the physical characteristics of the one-fluxon solution $\Phi^1$ presented in Tables 2–4. The number of fluxons (4.2) remains constant, that is, $N[\Phi^1] = 1$ at a change in the coefficient $a_2$. With an increase of parameter $a_2$, the total magnetic flow (2.6) for this solution approximates the value of this characteristic for a fluxon at infinite junction (4.1) ($\Delta\varphi = 1$). Moreover, the value of the function $\varphi(0)/\pi = 1$ does not change with a change in the amplitude. Total energy (2.5) decreases with an increase of the parameter $a_2$, which is shown in Fig. 3.

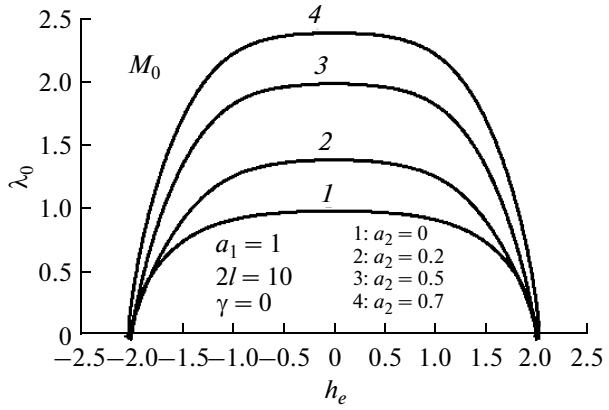


**Fig. 9.** Dependence of MEV on external field $h_e$ for $M_0$ at $\gamma = 0$ and at several values of parameter $a_2$.

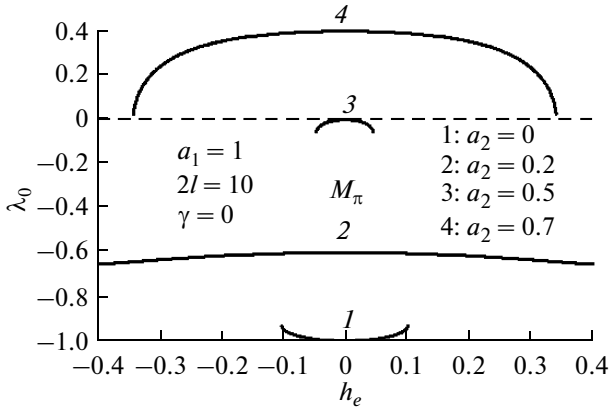


**Fig. 10.** Dependence of MEV on external field $h_e$ for CD $M_\pi$ at $\gamma = 0$ and different values of parameter $a_2$.

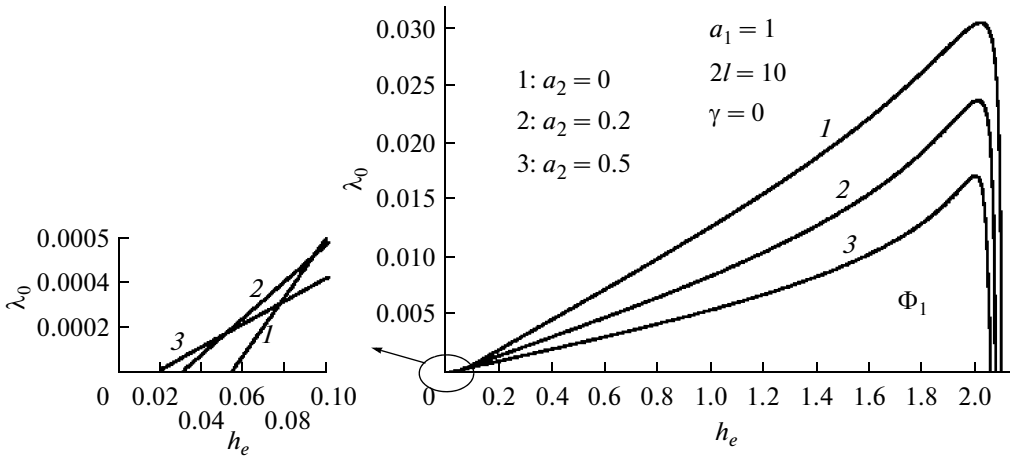


**Fig. 11.** Dependence of MEV on external field $h_e$ for fluxon solutions $\Phi^1$ at $\gamma = 0$ and $2l = 10$ for different values of parameter $a_2$.

With an increase of the external magnetic field $h_e$, more complicated stable fluxon states may exist. As an example, the derivatives of double-fluxon solutions $\Phi^2$ with $h_e = 2$ are shown in Fig. 6 for three positive values of the coefficient $\alpha_2$.

Note that the form of curves $\varphi'(x)$ changes qualitatively with $a_2 > 0.5$. There is symmetry relative to the vertical axis $x = 0$. The number of fluxons $N[\varphi]$ does not change: $N[\Phi^2] = 2$. With $a_2 = 0.5$, the curve $\varphi'(x)$ for solution $\Phi^2$ has the plateau ($\varphi'(x) \approx 2.2$) in the neighborhood of the point $x = \pm 1.9$. A further increase of parameter $a_2$ leads to the formation of two maxima of the eigenmagnetic field at the location of the plateau.

Each curve for $M_0$ has two zeros corresponding to the minimal and maximal values of the current $\gamma$. The distance between the zeros determines the field of the existence (stability) of the solutions. As an example, in Fig. 8, the effect of parameter $a_2$ on the field of the stable Meissner solution $M_0$ is shown: with an increase of $a_2$, the region $\Delta\gamma$ monotonically increases.

Figure 7 also shows the birth of stable states of $M_\pi$ from unstable ones at $a_2 > 0.5$. At $a_2 = 0.5$, the curve $\lambda_0(\gamma)$ for $M_\pi$ has a zero at the point $\gamma = 0$. Thereby, the value $a_2 = 0.5$ is a bifurcation for $M_\pi$ and $M_{\pm ac}$. In this case, the foregoing solutions coincide.

As parameter $\alpha_2 > 0.5$ increases, the graph $\lambda_0(\gamma)$ splits into three parts. A branch corresponding to the solution $M_\pi$ is situated in the half-plane $\lambda_0 \geq 0$.

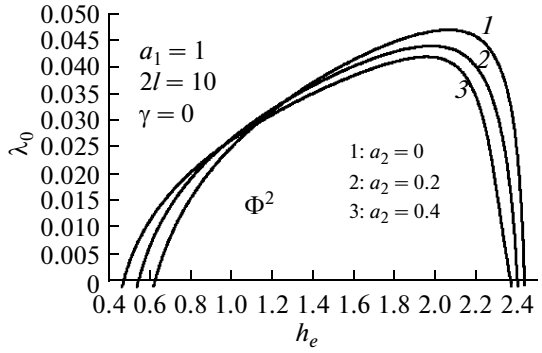


**Fig. 12.** Dependence of MEV on external field $h_e$ for fluxon solutions $\Phi^2$ at $\gamma = 0$ and $2l = 10$ for several values of parameter $a_2$.

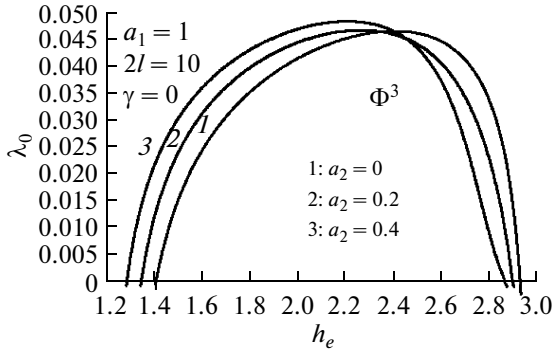


**Fig. 13.** Dependence of MEV on external field $h_e$ for fluxon solutions $\Phi^3$ at $\gamma = 0$ and $2l = 10$ for several values of parameter $a_2$.

### *4.3. MEV's Dependence on the External Field $h_e$*

Figure 9 shows the dependence $\lambda_0(h_e)$ for the Meissner solution $M_0$ with $\gamma = 0$ for several values of the parameter $a_2$. It is seen that $\lambda_0(h_e)$ increases with an increase of the parameter $a_2$, that is, the frequency of the junction's response to an arbitrarily small perturbation increases [10].

Figure 10 shows the transition from an unstable to a stable state of solution $M_\pi$, with a change of the coefficient $a_2$. Curve @1 corresponds to the solution in the conventional case ($a_2 = 0$). At values $a_2 < 0.5$, the value $\lambda_0(h_e) < 0$; that is, the state $M_\pi$, is unstable. With an increase of the parameter $a_2$, the graph $\lambda_0(h_e)$ rises upward. With $a_2 = 0.5$, the curve $\lambda_0(h_e)$ touches the straight line $\lambda_0 = 0$ at the point $h_e = 0$. Therefore, point $a_2 = 0.5$ is the point of bifurcation by parameter $a_2$. With $a_2 > 0.5$, the state $M_\pi$ is stable (curve @4 in Fig. 10). The solution $M_\pi$ is stable in the region $|h_e| < 0.34$ with $a_2 = 0.7$.

Where the tangent to curves $\lambda_0(h_e)$ is perpendicular to the $X$ axis, the bifurcation of a higher order (that is, $\lambda_n = 0$, $n > 0$) takes place.

Figures 11–13 demonstrate the dependence $\lambda_0(h_e)$ for the fluxon solutions $\Phi^1$, $\Phi^2$, and $\Phi^3$ for positive values of the parameter $a_2$. At $h_e < 0$, the $\Phi^n$ solutions have corresponding $\Phi^{-n}$ solutions, the graphs $\lambda_0(h_e)$ of which are symmetrical relative to the vertical axis. At $h_e = 0$, all fluxon solutions are unstable. For all shown solutions, the region of stability by $h_e$ shifts with an increase of $a_2$.

Thus, in the considered values of the coefficient $a_2$ $\varepsilon[0; 0.4]$, no substantial qualitative changes in the curves $\lambda_0(h_e)$ for the solutions $\Phi^1$, $\Phi^2$, and $\Phi^3$ appear.

## CONCLUSIONS

Mathematical modeling of statistical distributions of the magnetic flow in the long CD described by the double sine-Gordon equation has been performed. The stability of fluxon (vortical) fluxon solutions at changing parameters $h_e$ and the $\gamma$ for different values of the coefficient $a_2$, as well as their deformation, with a change in the parameter $a_2$ have been investigated. It is shown that taking parameter $a_2$ into account leads to the stabilization of the conventionally unstable Meissner solutions. New constant solutions that are absent in the conventional model with $a_2 = 0$ have been found.

## ACKNOWLEDGMENTS

We are grateful to I.V. Puzynin and T.P. Puzynina for their support and useful discussions.

This work was partially supported by the Program of Cooperation of the Joint Institute of Nuclear Research (JINR) with the Bulgarian research centers JINR—Bulgaria; and grant no. 39/2009 of Okhridski University, Sofia, Bulgaria. The work of Ye.V. Zemlyanaya and Yu.M. Shukrinov was partially supported by the Russian Foundation for Basic Research, grants 09-01-00770-a and 08-02-00520-a.

## REFERENCES


1. A. A. Golubov, M. Yu. Kypriyanov, and Ye. Il'ichev, The Current-Phase Relation in Josephson Junctions," *Rev. Mod. Phys.* **76**, 411 (2004).
2. V. V. Ryazanov, V. A. Oboznov, A. Yu. Rusanov, et al., Coupling of Two Superconductors Through a Ferromagnet: Evidence for a Junction," *Phys. Rev. Lett.* **86**, 2427 (2001).
3. A. A. Golubov and M. Yu. Kypriyanov, "The Current Phase Relation in Josephson Tunnel Junctions," *Pis'ma v ZhETF* **81** (7) 419—425 (2005).
4. K. K. Likharev, *Dynamics of Josephson Junctions and Circuits*, @ (Gordon and Breach, New York, 1986).
5. K. K. Likharev, *Introduction in Dynamics of Josephson Junctions* (Nauka, GRFML, Moscow, 1985) [in Russian].
6. K. K. Likharev, "Superconducting Weak Bonds: Stationary Processes," *Usp. Fiz. Nauk* **127** 185 (1979).
7. A. Buzdin and A. E. Koshelev, "Periodic Alternating 0-and -π–Junction Structures As Realization of φ – Josephson Junctions," *Phys. Rev. B* **67@,** 220504 (2003).
8. N. Hatakenaka, K. Takayanagi, Y. Kasai, and S. Tanda, "Double Sine-Gordon Fluxons in Isolated Long Josephson Junction, *Physica, B* **284–288**, 563–564 (2000).
9. M. Nishida, K. Murata, T. Fujii ?., and N. Hatakenaka, "Time Dilation of a Bound Half-Fluxon Pair in a Long Josephson Junction with a Ferromagnetic Insulator," *Phys.Rev. Lett* **99**, 207004 (2007).
10. Yu. S. Gal'pern and A. T. Filippov, "Bound States of Solitons in Inhomogenous Josephson Junctions with a Ferromagnetic Insulator," *ZhETF* **86** (4) 1527 (1984); *Sov. Phys. JETP*, No. 59, 894 (1984).
11. A. D. Polyanin and V. F. Zaitsev, *Handbook on Nonlinear Differential Equations. Applications in Mechanics, Exact Solutions* (Nauka FML, Moscow, 1993) [in Russian].
12. E. P. Zhidkov, G. I. Makarenko, I. V. Puzynin, et al., "A Continuous Dialogue of the Newtonian Method in Nonlinear Problems of Physics," *ECha YA* **4** (1) 127 (1973).
13. K. V. Puzynin, K. V. Amirkhanov, E. V. Zemlyanaya, *et al.*, Generelized Continuous Analogue of the Newtonian Method for Numerical Study of Some Nonlinear Quantum-Field Models," *ECha YA* **30** (1) 210—265 (1999).
14. K. V. Puzynin, T. P. Boyadeyuiev, S. I. Vinitskii, *et al.*, Methods of Computational Physics for Study of the Models of Complicated Physical Processes," *ECha YA* **38** (1) 144—232 (2007).
15. M. S. Kaschiev, V. A. Kaschieva, V. G. Makhan'kov, *et al.*, "Numerical research of Stability and Bifurcation Points of Bound Static States of Fluxons in a Circular Josephson Junction with Micro Inhomogeneity," *oobshchenie OIYaI* 11, 84–832 (1984).
16. V. V. Ermakov and K. N. Kalitkin, "The Optimal Step and Regularization of the Newtonian Method," *ZhVMiMF*, No. 21, 491 (1981).
17. Yu. S. Zav'yalov, B. I. Kvasov, and V. L. Miroshnichenko, *Methods of Spline-functions* (Nauka GRFMLm Nisciwm 1980) [in Russian].
18. N. S. Berezin and E. P. Zhidkov, *Metody vychislenii* (Nauka, Moscow, 1960) [in Russian].
19. TRIDIB – translation of the ALGOL procedure BISECT, Num. Math. 9, 386–393(1967) by Barth, Martin, and Wilkinson. Handbook for Auto. Sotr., vol.ii–linear algebra, 249–256(1971).
20. C. S. Owen and D. J. Scalapino, "Vortex Structure and Critical Currents in Josephson Junctions," *Phys. Rev. Lett* **164** (2)538–544 (1967).
21. A. N. Vystavkin, Yu. F. Drachevskii, V. P. Koshelei, and I. L. Serpuchenko, "Detection of Static Bound States of Fluxons in the Distributed Josephson Junctions with Inhomogenity, *Fiz. Nizk. Temp.* (Kiev) **14** (6) 646 (1988).